Electronic Supplementary Information (ESI) for:

Strain Rate Dependent Nanostructure of Hydrogels with Reversible Hydrophobic Associations During Uniaxial Extension

Chao Wang,[a] Clinton G. Wiener,[a] Masafumi Fukuto,[b] Ruipeng Li,[b] Kevin G. Yager,[c] R. A. Weiss,[*a] Bryan D. Vogt[*a]

[a] Department of Polymer Engineering, University of Akron, Akron, OH 44325, USA.

[b] National Synchrotron Light Source II, Brookhaven National Laboratory, Upton, New York 11973, USA

[c] Center for Functional Nanomaterials, Brookhaven National Laboratory, Upton, New York 11973, USA

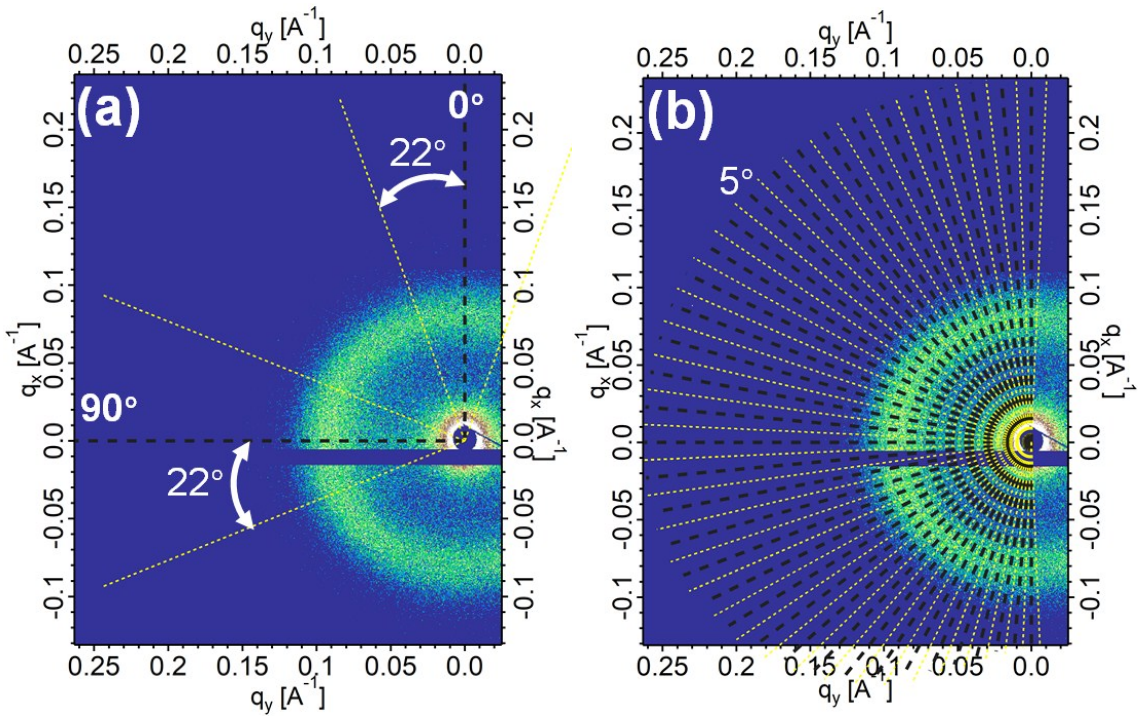

Figure S1. 2-D scattering pattern of a DF10 hydrogel after stretching at 8.4%/s to ~75% strain. The yellow dashed lines show (a) the azimuthal range for the sector averages (± 22°) (b) sector averages (± 2.5°) used to determine the scattering intensity as a function of azimuthal angle.

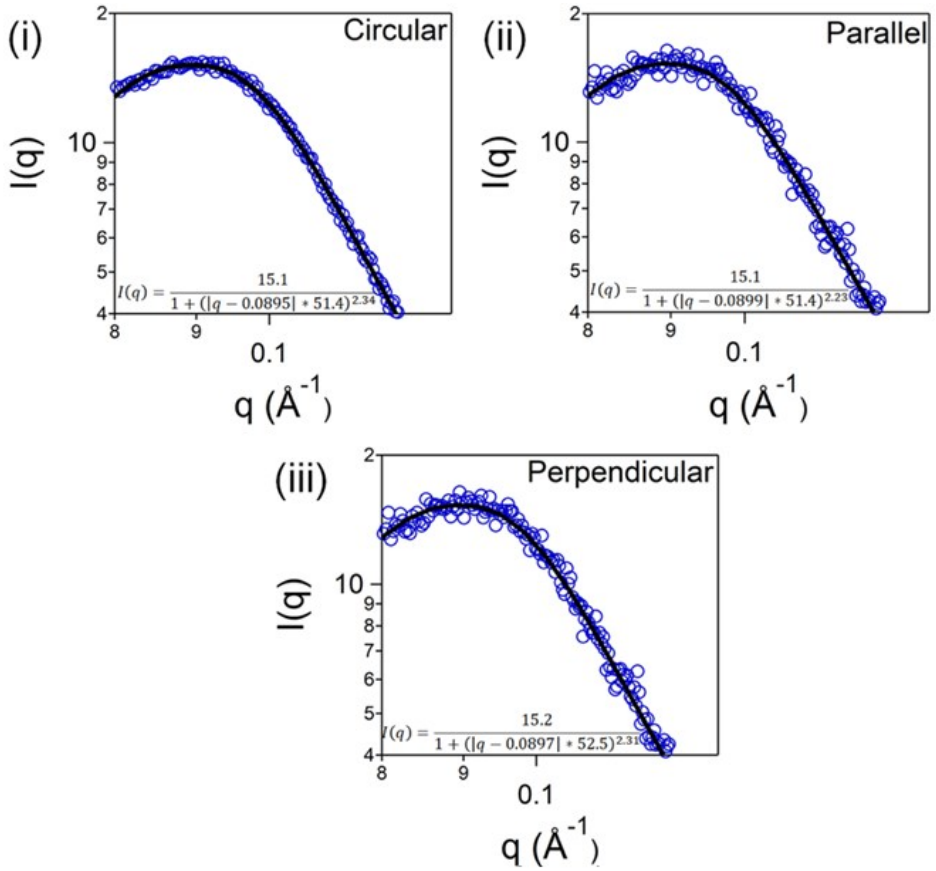

Figure S2. Comparison of the azimuthally averaged 1-D scattering pattern of a DF10 hydrogel before elongation using (i) all azimuthal angles with a comparison to the sector averages (± 22°) that are (ii) parallel and (iii) perpendicular to the stretching direction. The black curve is the best fit using the broad peak model. The fit parameters are almost indistinguishable in all three cases as expected for the isotropic sample. The error bars in the scattering data were omitted for clarity.

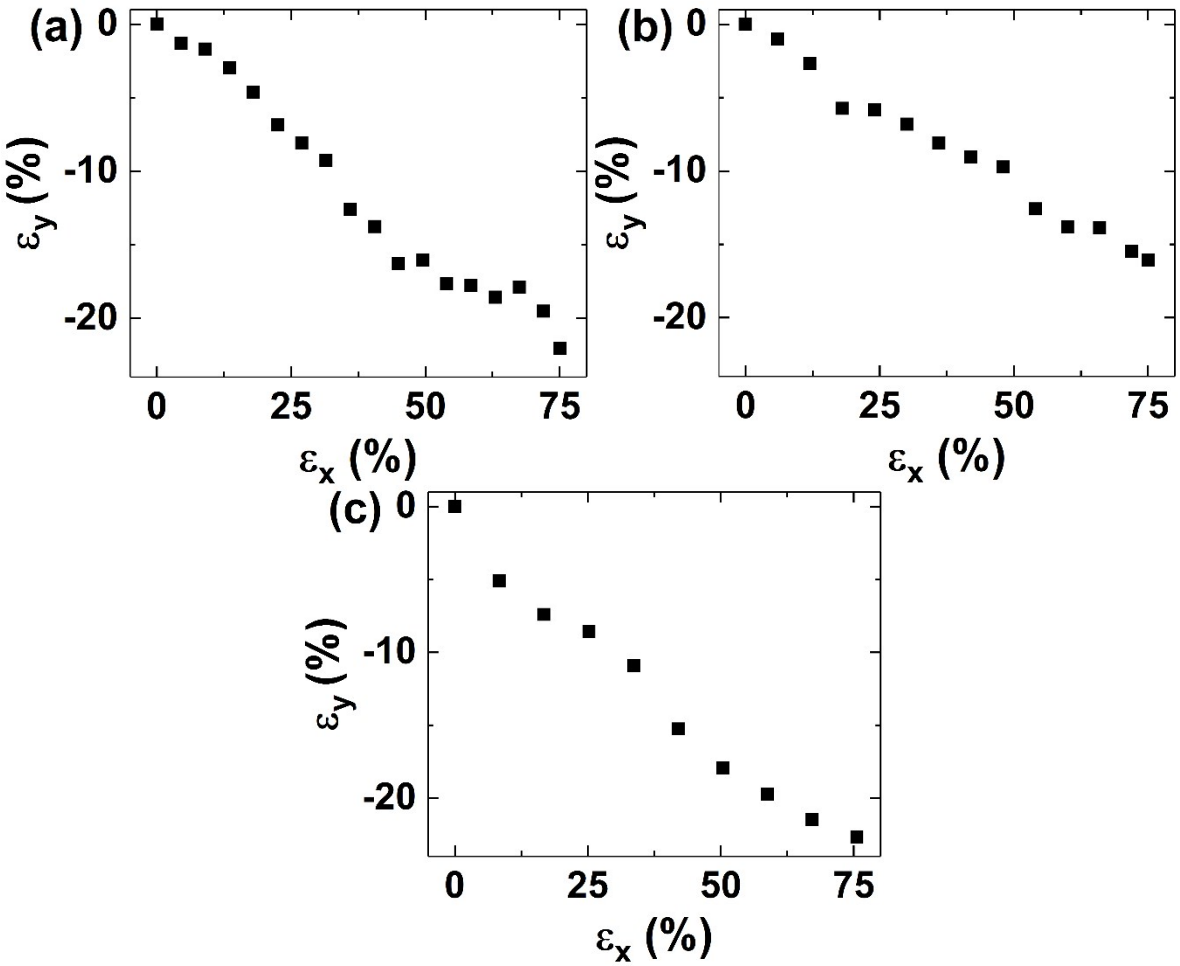

Figure S3. Macroscopic strains of the DF10 hydrogel in the direction parallel (ε_x) and perpendicular (ε_y) to the uniaxial extension at (a) 0.15%/s (b) 1.5%/s and (c) 8.4%/s.

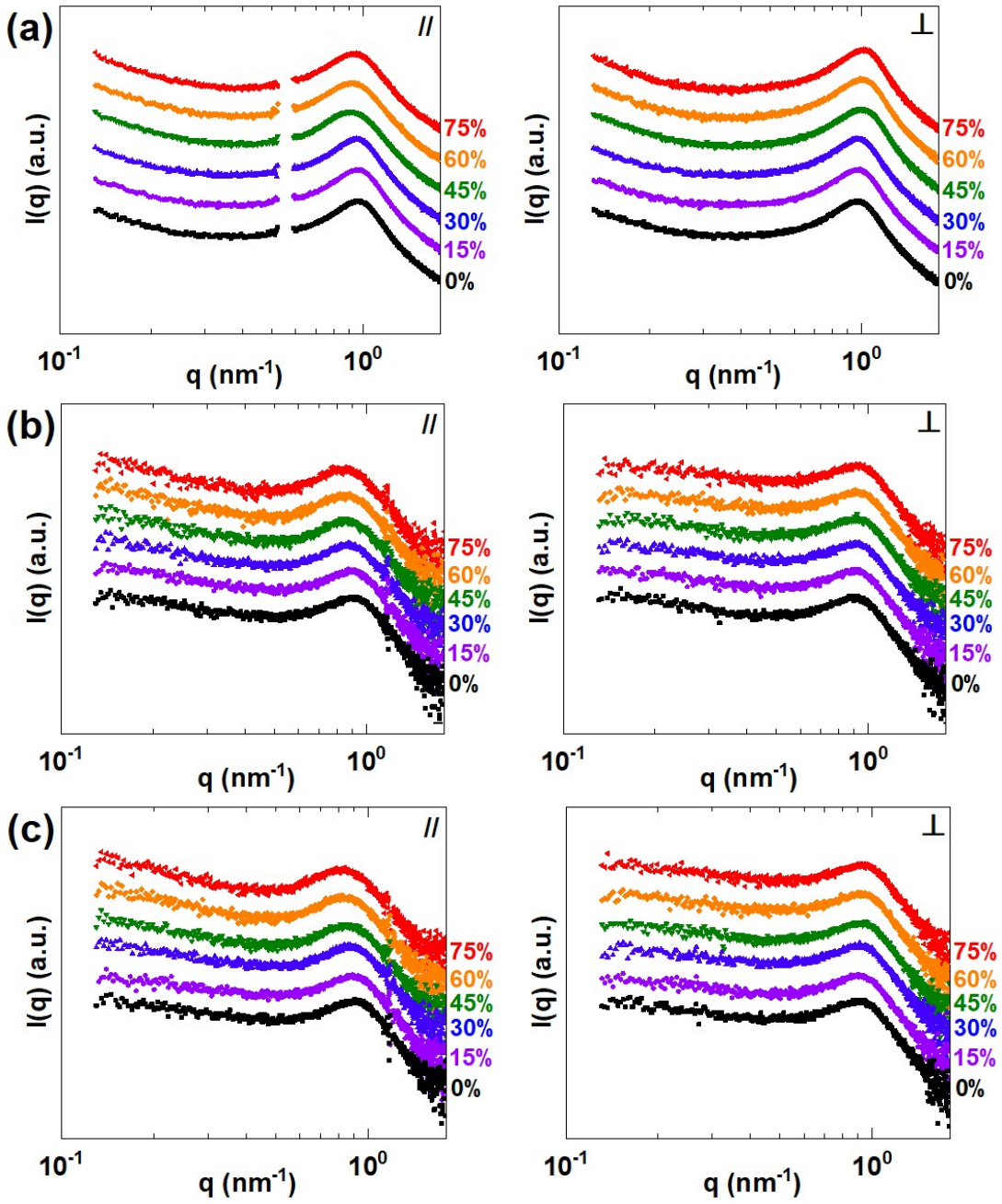

Figure S4. Evolution of the 1-dimensional scattering profiles for the DF10 hydrogels under uniaxial extension at strain rates of (a) 0.15%/s (b) 1.5%/s and (c) 8.4%/s. The strain corresponding to each curve is listed to the right of the profile.

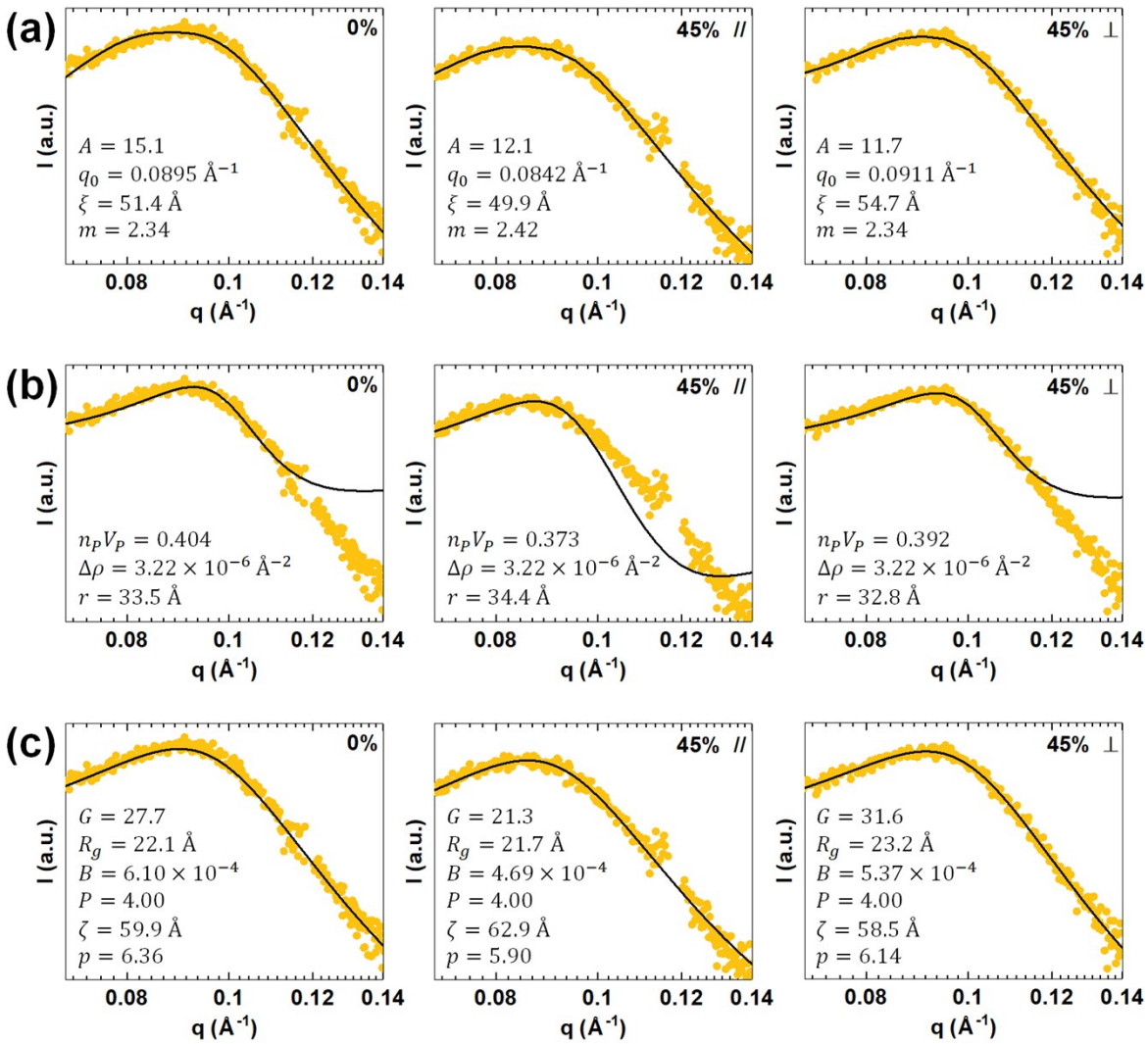

Figure S5. Representative fits of the peak in the 1-D profiles for the (a) BP, (b) HS, and (c) BC models at 0% and ~45 % engineering strain when the hydrogel was stretched at 8.4 %/s. The best fit parameters from the model are included in the appropriate panel. All three models reasonably fit the experimental scattering data although the HS model begins to fail at high q.

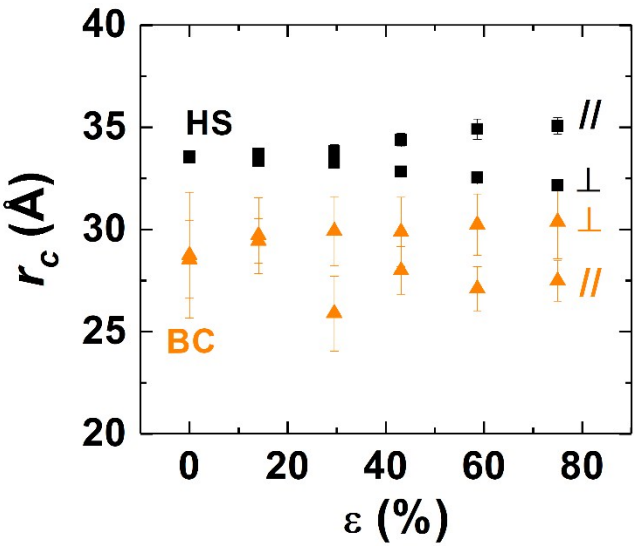

Figure S6. Comparison of the domain radius (r_c) evolution during uniaxial stretching at a strain rate of 8.4%/s obtained from the (■) HS and (▲) BC model.

Figure S7(a)-(c) illustrates how the amplitude of the correlation peak in the scattering data (Figure 2) as fit by the Lorentzian, *A*, depends on the azimuthal angle. This fit has been corrected for the background. Before extension, the distribution of nanodomains was isotropic, so *A* was independent of the azimuthal angle. Irrespective of strain rate, extension of the hydrogel reduced *A* due to decreased thickness that decreases the number of scatterers probed. At large strains, e.g., 45% and 75%, a maximum in scattered intensity at the azimuthal angle normal to the stretching direction is observed. This intensity difference can be correlated to the number density of scatterers probed by the beam. Either the FOSA nanodomains are less correlated along the stretching direction or there are less FOSA nanodomains present. This later case is consistent with the anisotropic change in D_i; an increase in D_i will decrease the number density of scatterers and increasing strain rate leads to greater anisotropy in the amplitude of the correlation peak. This behavior is also consistent with the decreased volume fraction of FOSA domains from the fits to the HS model.

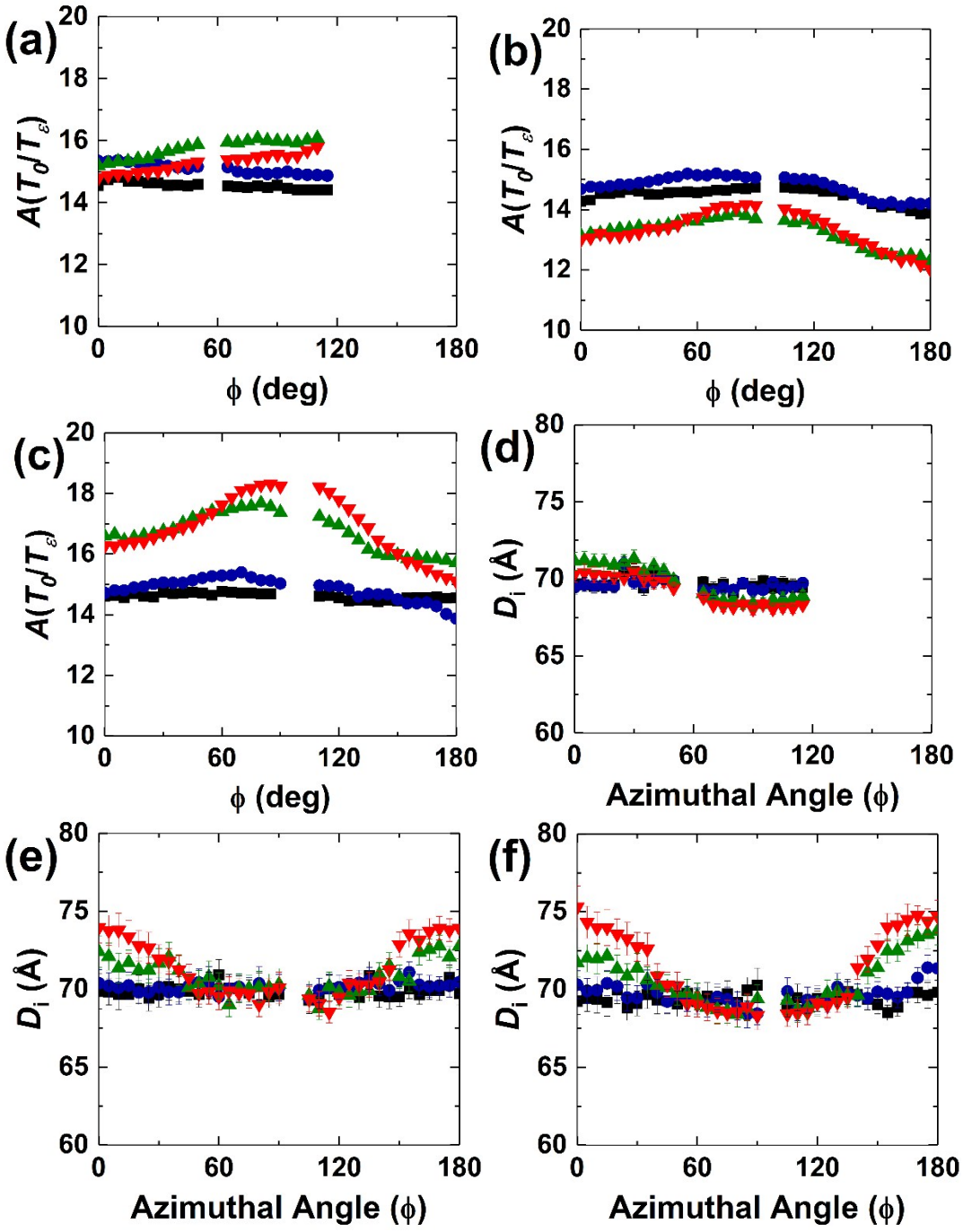

Figure S7. The azimuthal angle (ϕ) dependence of the (a)-(c) normalized Lorentzian amplitude (A) and (d)-(f) interdomain spacings (D_i) at strains of (■) 0%, (●) ≈15%, (▲) ≈45% and (▼) ≈75% during uniaxial extension at strain rates of (a and d) 0.15%/s, (b and e) 1.5%/s, and (c and f) 8.4%/s. For (a)-(c), the standard deviations are in the range of 5%-7% and the error bars are omitted for clarity.

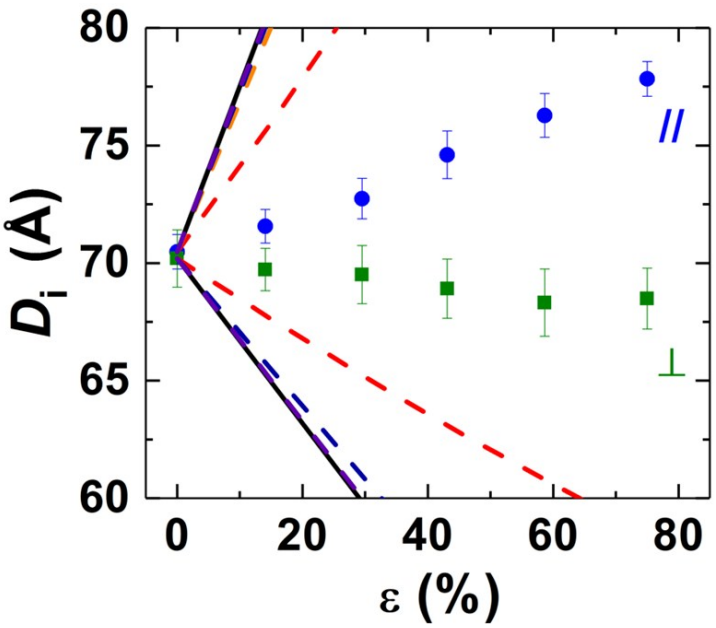

Figure S8. The interdomain spacings (D_i) for the DF10 hydrogel parallel (//) and perpendicular (⊥) to the stretching direction at strain rate of 8.4 %/s from the BP model. Impact of functionality (f) on predicted changes for the phantom network model (dashed lines) with f = 4 (red), 20 (orange), 50 (dark blue) and 138 (purple). The affine model prediction is shown in the solid black line.

The three stretched exponentials model is shown in Equation (S1)

$$\frac{\sigma(t)}{\sigma_0} = A_1 e^{-\left(\frac{t}{\lambda_1}\right)^{\beta_1}} + A_2 e^{-\left(\frac{t}{\lambda_2}\right)^{\beta_2}} + (1 - A_1 - A_2) e^{-\left(\frac{t}{\lambda_3}\right)^{\beta_3}} \qquad (S1)$$

where $\sigma(t)/\sigma_0$ is the normalized stress at time t, λ_1, λ_2 and λ_3 are the characteristic relaxation time when the value of a single stretched exponential is 1/e, β_1, β_2 and β_3 describe the relaxation time distribution, A_1 and A_2 are adjustable constants between 0 and 1. The fitted parameters are shown in Table S1.

Table S1. Fitted parameters from three stretched exponentials.

Fitted parameters	λ_1	β_1	λ_2	β_2	λ_3	β_3
	21.6	0.571	480	0.600	1.457×10^7	0.563

The Generalized Maxwell Model is shown in Equation (S2)

$$\frac{\sigma}{\sigma_o} = \sum_{i=1}^{N} c_i e^{-t/\tau_i} \qquad (S2)$$

where c_i = fractional contribution of the i^{th} Maxwell model and τ_i = relaxation times. The Maxwell element N = 1 to 5. The fitted curves are shown in Figure S9 and the fit parameters are shown in Table S2. $\sum_{i=1}^{N} c_i$ should be 1 for the model to well represent the data. As shown in Table S2, only when some very long relaxation time processes are presented in the fitting (N = 3 to 5), a reasonable fit occurs with $\sum_{i=1}^{N} c_i \approx 1$.

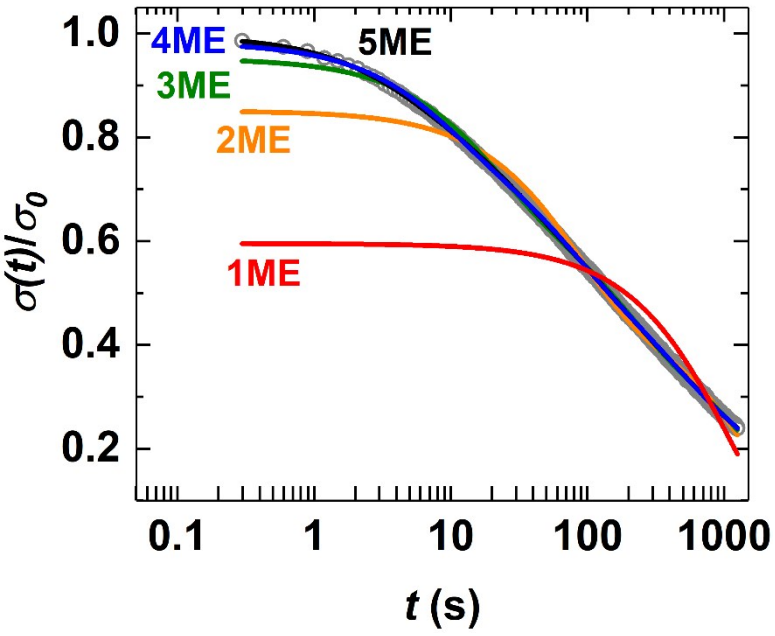

Figure S9. Fitted curves using Generalized Maxwell Model with residual stress and N = 1 to 5 on the stress relaxation data of DF10 after a 75% step strain.

Table S2. Fitted parameters from Generalized Maxwell Model with residual stress and N = 1 to 5 for the stress relaxation of the DF10 hydrogel after 75% step strain.

Maxwell Element	1 ME Model		2 ME Model		3 ME Model		4 ME Model		5 ME Model	
	c_i	τ (s)	c_i	τ (s)	c_i	τ (s)	c_i	τ (s)	c_i	τ (s)
1	0.595	1093	0.385	78.6	0.258	18.5	0.176	8.18	0.103	3.96
2			0.466	1732	0.283	167	0.222	56.7	0.163	20.6
3					0.410	2259	0.250	329	0.211	95.1
4							0.333	3530	0.325	642
5									0.194	1.14E+28
Σc_i	0.595		0.851		0.951		0.981		0.996	
COD	0.8474		0.9925		0.9994		0.9998		0.9999	

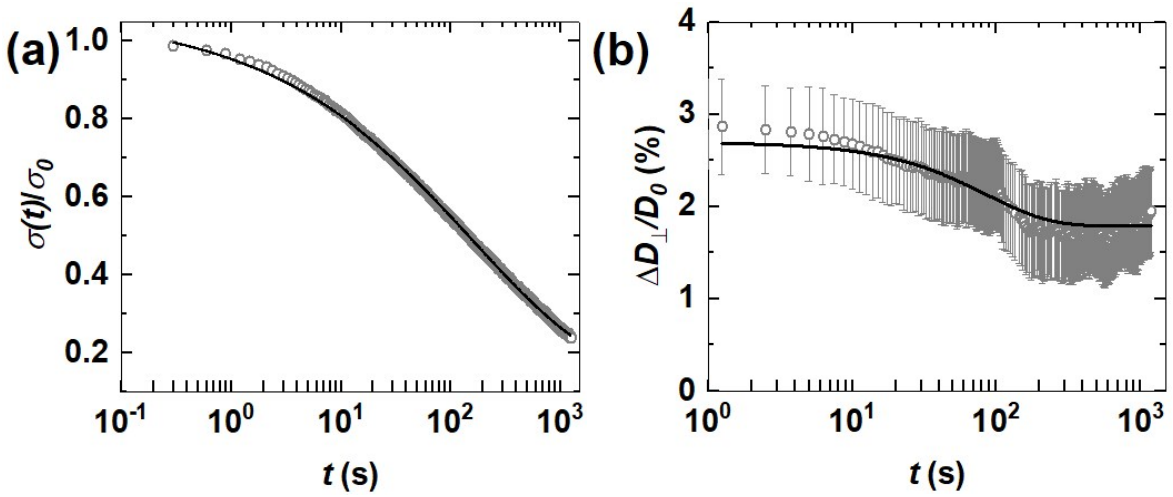

Figure S10. (a) Stress relaxation response for the DF10 hydrogel following a step strain of 75%. (b) The percentage change of $D_\perp$ comparing to the unstretched state ($\Delta D_\perp/D_0$) during the stress relaxation process in (a). The solid lines are the fit to Equation (11).